JTTEE5 18:50–57
DOI: 10.1007/s11666-008-9282-1
1059-9630/$19.00 © ASM International

Ultrafast Thermal Plasma Preparation of Solid Si Films with Potential Application in Photovoltaic Cells: A Parametric Study

Behnam Mostajeran Goortani, François Gitzhofer, Etienne Bouyer, and Mehdi Mousavi

(Submitted March 23, 2008; in revised form July 9, 2008)

An innovative method, namely ultrafast plasma surface melting, is developed to fabricate solid films of silicon with very high rates (150 cm^2/min). The method is composed of preparing a suspension of solid particles in a volatile solvent and spreading it on a refractory substrate such as Mo. After solvent evaporation, the resulting porous layer is exposed to the flame tale of inductively coupled RF plasma to sinter and melt the surface particles and to prepare a solid film of silicon. It is shown that by controlling the flow dynamics and heat transfer around the substrate, and managing the kinetic parameters (i.e., exposure time, substrate transport speed, and reaction kinetics) in the reactor, we can produce solid crystalline Si films with the potential applications in photovoltaic cells industry. The results indicate that the optimum formation conditions with a film thickness of 250-700 μm is when the exposure time in the plasma is in the range of 5-12.5 s for a 100 × 50 mm large layer. By combining the Fourier's law of conduction with the experimental measurements, we obtained an effective heat diffusivity and developed a model to obtain heat diffusion in the porous layer exposed to the plasma. The model further predicts the minimum and maximum exposure time for the substrate in the plasma flame as a function of material properties, the porous layer thickness and of the imposed heat flux.

Keywords heat diffusivity, silicone, solid film, thermal plasma

1. Introduction

With the current environmental status and the forthcoming restrictions in fossil energy, the need to develop renewable and clean sources of energy is obvious. Converting the sun energy to electricity using silicon photovoltaic cells is one of the conventional methods in this respect, which has a high deployment opportunity (Ref 1, 2). There are various laboratory and industrial routes for the production of silicon films suitable for photovoltaic cells, namely thermal plasma spraying, chemical vapor deposition (CVD), physical vapor deposition (PVD), hot wire sputtering, and slicing techniques. However, a current challenge in this path is to overcome the restrictions concerning the rate of production and consequent extra costs (Ref 3-5).

Thermal plasma spraying (RF plasma methods or hybrid DC-RF thermal plasma) seems to be a potential method for the ultra high rate of silicon deposition. Chae et al. (Ref 5), for example, have succeeded to use thermal plasma chemical vapor deposition (TPCVD) to deposit Si on SiO_2 and c-Si substrates with rates of production in the order of several nanometers per second.

There are various factors that affect the quality of the film during the formation of films and coatings by thermal plasma. Substrate temperature, distance to the torch, plasma gas, reactor pressure, and plasma power are the most important ones studied so far in the literature (Ref 6-9). These factors affect directly the photovoltaic activity of the films by changing the level of impurities, the microstructure of the film, the porosity, and the crystalline structure.

In other conventional methods of solid film formation such as CVD and PVD processes, the films are formed by condensing the vapors on a substrate. Sasaki et al. (Ref 10), for example, studied the effect of substrate temperature on Si film properties and showed that at the optimum temperature of 85 °C microcrystalline Si grows on the amorphous Si layer while at higher or lower temperatures the structure is either porous or half amorphous half crystalline. Slicing methods are the most conventional methods of Si film production. In these methods, the film is formed by mechanical cutting of a solid Si bar. However, the waste of materials during production is too much.

An important weakness of all of the methods found in the literature is that either the rate of production is very low (several orders of magnitude less than 1 cm^2/min) or the waste of materials is too important. Another common feature is that those methods are batch in nature. The objective of this study is to introduce an innovative method in thermal processing of materials, namely ultrafast plasma surface melting (UPSM), which is used to

Behnam Mostajeran Goortani and **François Gitzhofer**, Université de Sherbrooke, Sherbrooke, Canada; and **Etienne Bouyer** and **Mehdi Mousavi**, Commissariat à l'Énergie Atomique (CEA), Grenoble, France. Contact e-mail: Francis.Gitzhofer@USherbrooke.ca.

fabricate solid silicon films with rates of the order of several cm^2/min and may be used to continuously produce Si films for photovoltaic cells industry. In the experimental work of this study, it will be demonstrated how various process parameters such as relative movement of the substrate under the plasma and plasma torch-substrate distance change the thickness of the film. Furthermore, the theoretical part of this work introduces a model which predicts the diffusion of heat into the porous layer during the formation process and so the minimum and maximum allowable exposure time.

2. Experimental

2.1 Experimental Set-up

Figure 1 shows the reactor for the fabrication of silicon films. The reactor was composed of a horizontal water cooled cylinder with a diameter of 50 cm and a length of 1 m at top of which a PL-50 RF plasma torch (Tekna Plasma Systems, Sherbrooke, Canada) was installed. The hot plasma gases (Ar as the central and He-Ar-H_2 as the sheath) entered the reactor through the torch. The substrate was placed between 8 and 15 cm from the torch nozzle and had the capability of horizontal movement inside the reactor.

2.2 Innovative Film Formation Process: Plasma Surface Melting

Film formation process is described according to Fig. 2 (Ref 11). In this process, first a suspension of solid particles in solvent (such as methanol) is deposited on a Mo substrate.* Consequently, the solvent is evaporated and a dried layer of porous material is formed. The layer is then exposed to the plasma flame inside the reactor according to Fig. 2(a). After exposition to this high heat flux source, depending on plasma parameters and time of exposition, the particles are gradually sintered or melted together to form a porous or a solid layer according to Fig. 2(b).

2.3 Plasma Parameters

Table 1 presents the plasma operating parameters used during the experiments. Hydrogen was used in the sheath to prevent unwanted reactions (purifying gas) (Ref 12, 13) and to modify the photovoltaic properties of silicon by preventing the dangling bonds (defects) present in the Si structure (Ref 3, 5, 14-17). The plasma power was set between 20 and 24 kW depending on the particles' size. The pressure inside the reactor was kept to the minimum amount (130-150 Torr) to help the degasification during the melting and prevent the unwanted reactions. At higher pressures, the film was not formed or it was very porous.

The feed was a mixture of 48% silicon powders provided by AEE (−100 μm, electronic grade) and the balance being HC-Stark (grade AX-05, −8 μm, 99.995% purity, maximum percentage level of impurities: Fe, 0.001; Al, 0.001; Ca, 0.0005; other, 0.0025). Figure 3 shows an SEM image of the feed and shows that it is composed of irregular shaped particles with sharp edges.

2.4 Characterizations and Experimental Measurements

Scanning electron microscopy (SEM), X-ray spectroscopy (EDS), and X-ray diffractometry (XRD) were used to characterize and to measure the electrical resistivity of such films.

2.4.1 The Microstructure of the Film. Figure 4 shows the microstructure of the UPSM film (23.5 kW, 150 Torr, 48% AEE powder, and 6 cm substrate distance). Figure 4 (left) is a SEM image of the film surface. It shows a uniform solid zone and some color dots on the surface. The uniform zone shows a microstructure without defects on the surface. While the color dots represent the impurities such as nanoparticles of oxide and nitride of silicon (as is shown by the XRD results of the next section). Figure 4 (right), on the other hand, shows the cross-sectional SEM image of the sample. From this figure, the film cross section is composed of three layers, namely top layer, intermediate bulk layer, and porous part. The upper layer, the non-pure layer, which is typically between 0 and 100 nm, is composed of Si, O, and N, as measured by energy dispersive X-ray spectroscopy (EDS) installed on a high-resolution Hitachi S-4700 electronic microscope, which shows that the surface of the film has been attacked by trace amount of the elements present in the reactor. The intermediate solid layer, which is pure silicon as measured by the same EDS, has a thickness of about 100 μm. In fact, it is this intermediate layer that has the potential of having photovoltaic activity. Finally, the lower porous layer, which has a thickness of 250-350 μm, represents the partially sintered and non-melted particles.

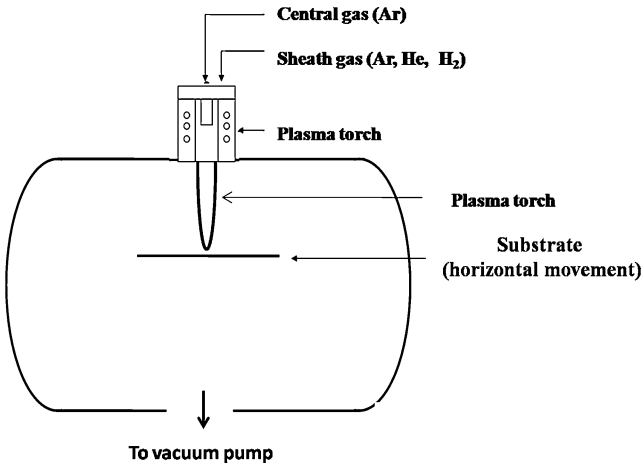

Fig. 1 Schematic of the experimental set-up for the fabrication of Si films

*Any refractory material stable in high temperature reductive environment can be used instead of Mo substrate.

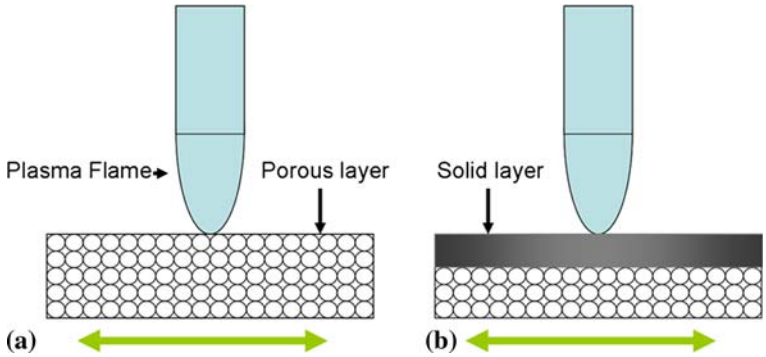

Fig. 2 The innovative process of UPSM (Ref 11)

Table 1 Plasma operating parameters for silicon film fabrication by UPSM method

Process parameter	Value
Plasma gas and flow rate	
Central gas	Ar, 22.5 slpm
Sheath gas	Ar (10 slpm), He (200 slpm), H_2 (3%)
Substrate transport speed	5-10 mm/s
Plasma power plate	20-24 kW
Reactor pressure	150-200 Torr
Substrate distance	7-15 cm

2.4.2 The Crystalline Structure. X-ray diffractometry measurements (Fig. 5) showed that the prepared films are completely crystalline and the resulting pattern corresponds to the standard crystalline pattern of silicon (JCPDS # 00-027-1402 Si). The other peaks at 35 and 50 correspond to the impurities at the surface of the film, e.g. Si_3N_4 and SiO_2.

2.4.3 Effect of the Substrate Distance. By decreasing the substrate distance from the torch, the scanned area by the high heat flux increases, consequently a film of larger surface area is formed. Table 2 shows the surface area of the formed film as a function of the substrate distance. The experiments were performed with a 6 × 6 cm substrate. According to this table, by decreasing this distance from 15 to 8 cm, the formed surface area increases from 12 to about 36 cm^2.

3. Theory

In this section, a simple mathematical model is proposed to obtain the transient response of the porous layer exposed to the plasma flame. Consequently, the experimental results of maximum and minimum exposure time (Section 3.1) have been used to obtain an effective heat diffusion coefficient for the porous layer and to predict the minimum and maximum allowable exposure time as a function of film thickness and material properties.

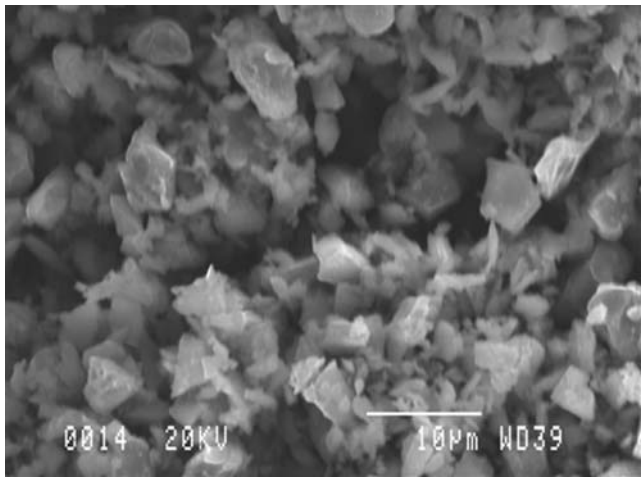

Fig. 3 SEM image of the raw powder feed (HC-Stark, AX-05 Si metal powder)

3.1 Hypotheses and Assumptions

The process is composed of two stages, before the temperature reaches the melting temperature of silicon and after melting the porous layer, respectively. Our hypothesis is that the second stage (melting process) is fast compared to the first stage. Consequently, the process can be approximated only by considering the transient heat diffusion into the porous layer. Furthermore, the following assumptions are made:

1. Constant physical properties for the porous layer during exposure to the plasma.
2. The total heat flux (convective and radiant) into the porous layer is constant and equal to 5 kW as measured by a simple calorimeter.
3. The porous layer on the other end is completely isolated.

3.2 Modeling the Diffusion of Heat into a Porous Layer

The objective here is to find the transient temperature distribution of the porous layer, which is a rectangular slab. Figure 6 schematically depicts the slab. This slab is

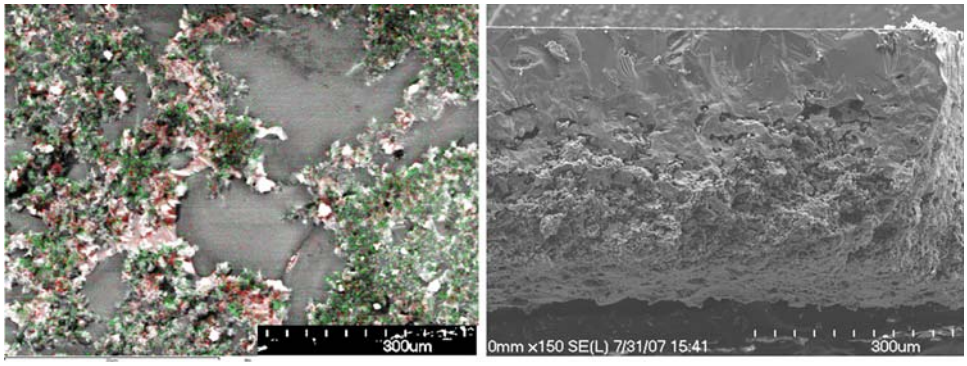

Fig. 4 SEM image of silicon film: (a) microstructure of the film surface and (b) cross-sectional view

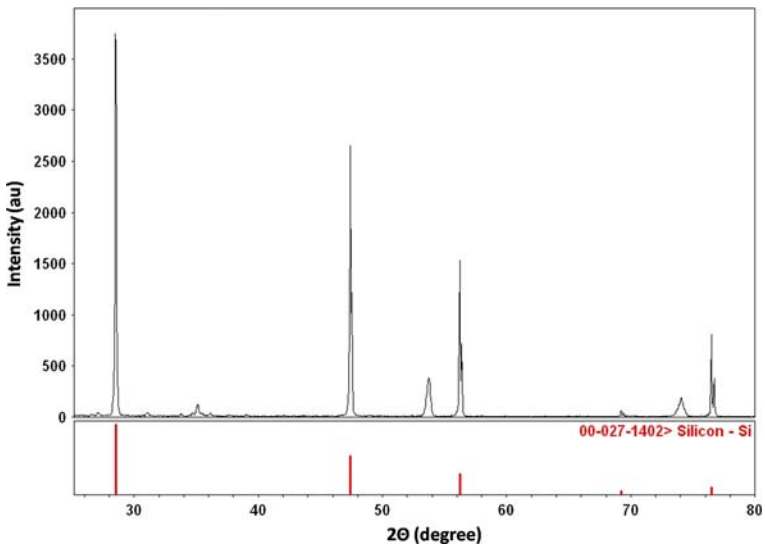

Fig. 5 X-ray diffractometry measurement of the prepared silicon films

Table 2 The formed surface area as a function of distance of the substrate to the torch

Distance, cm	15	12	10	8
Surface area, cm^2	12	24	30	36

heated from one side ($x = 0$) by the plasma flame and is insulated on the other side ($x = a$).

The transient response of this porous layer can be considered to be in the form of (Ref 18):

$$\partial t/\partial \theta = \alpha(\partial^2 t/\partial x^2) \quad \text{(Eq 1)}$$

where $\theta = \theta(t, x)$ is the exposure time, α is the thermal diffusivity, and x is the distance from the surface exposed to the high heat flux source.

This classical heat transfer problem should be solved with the following initial and boundary conditions:

$$\text{I.C.} \quad \theta(0, x) = 300\,\text{K}$$
$$\text{B.C.1} \quad \partial\theta(t, 0)/\partial x = 5000$$
$$\text{B.C.2} \quad \partial\theta(t, a)/\partial x = 0$$

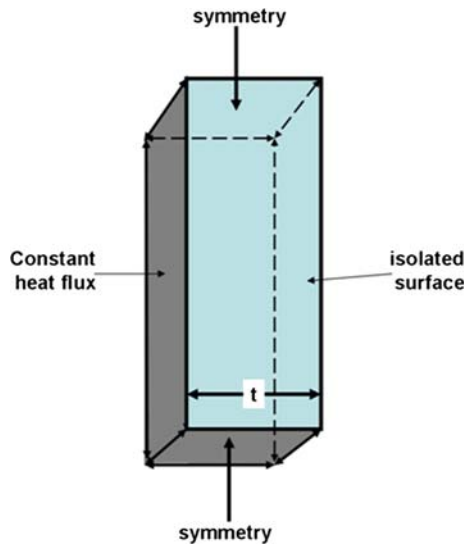

Fig. 6 Calculation domain for predicting the temperature distribution in the porous layer

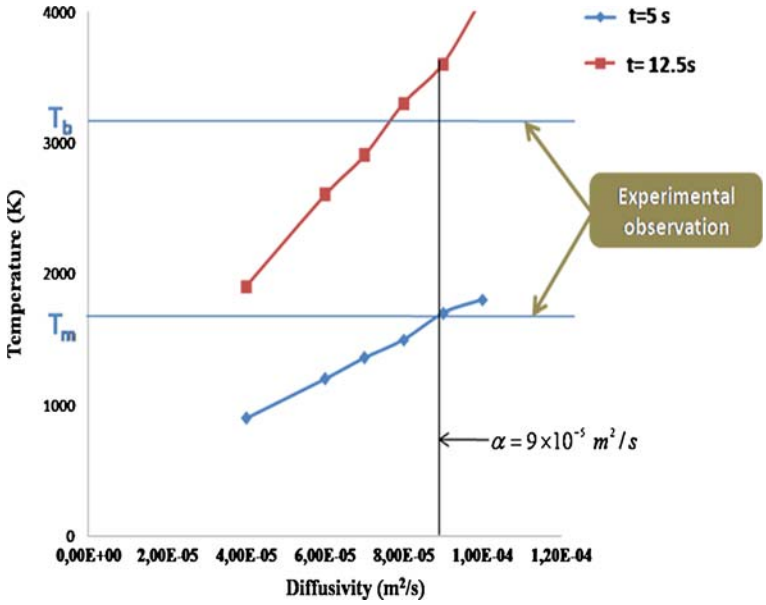

Fig. 7 Surface temperature predictions as a function of diffusivity and comparison with the experimental data

3.3 Obtaining the Effective Heat Diffusivity of the Porous Layer

There may be some analytical solutions for Eq 1 (e.g., see Ref 19) with the previously mentioned initial and boundary conditions, but because of the repetitive use of the equation in this section, a simple numerical solution is proposed using Matlab^{TR} 7.0.4 and the temperature distribution in the slab is derived. In Eq 1 the only unknown parameter is the diffusivity $\alpha = k/\rho c_p$. For our experiments, this value depends on the physical properties of the silicon, the porosity, and the architecture of particles in the porous layer. To find this value, the transient heat equation was solved for various values of α and by comparison with the experimental data (the minimum and maximum exposure time, Section 3.1), the correct value of α was obtained. Figure 7 shows this concept in more details.

From this figure the correct value for diffusivity that corresponds to boiling point ($T_b = 3200$ K) and melting point ($T_m = 1400$ K) of Si is:

$$\alpha = 9 \times 10^{-5}\,\mathrm{m^2/s} = 0.9\,\mathrm{cm^2/s}$$

4. Discussion

In this section we try to find more details about two important factors that directly affect the flow dynamics and heat transfer to the substrate: (a) to determine the process envelope for allowable exposure times of the porous layer under the plasma and (b) to reduce the turbulency level of the plasma gases by injecting He in the sheath gas.

4.1 Minimum and Maximum Exposure Time

The most critical parameter of film formation is to adjust the residence time of the substrate inside the plasma by setting the velocity of the substrate holder in the reactor. This parameter determines the exposure time of the porous layer to the plasma flame. According to the experimental observations, the optimum conditions of film preparation lie within a minimum and maximum exposure time. At exposure times outside these two limits, the film either does not form or is overmelted resulting with a poor quality. At exposure times within these limits, the film is either porous or is solid.* Our observations indicate that, for the fabrication of silicon film, the maximum and minimum scanning speed of the substrate ν_{max} and ν_{min} should be 10 and 4 mm/s respectively. These values correspond to minimum and maximum exposure time θ_{min} and θ_{max} of:

$$\theta_{min} = d/\nu_{max} = \frac{50\,\mathrm{mm}}{10\,\mathrm{mm/s}} = 5\,\mathrm{s}$$

$$\theta_{max} = d/\nu_{min} = \frac{50\,\mathrm{mm}}{4\,\mathrm{mm/s}} = 12.5\,\mathrm{s}$$

Now we can use these values to predict the minimum and maximum exposure time for other values of thickness of the porous layer. This work has been performed by using the previous model of Section 2.3 and allows us to predict the exposure time for various thicknesses of porous film. The results are presented in Fig. 8.

From this figure, as the thickness of the porous layer increases, the gap between the t_{max} and t_{min} increases. In

*Substrate speed, substrate to torch distance, plasma power, and relative velocity of plasma gas over the substrate are critical parameters that determine if we obtain sintered or melted silicon.

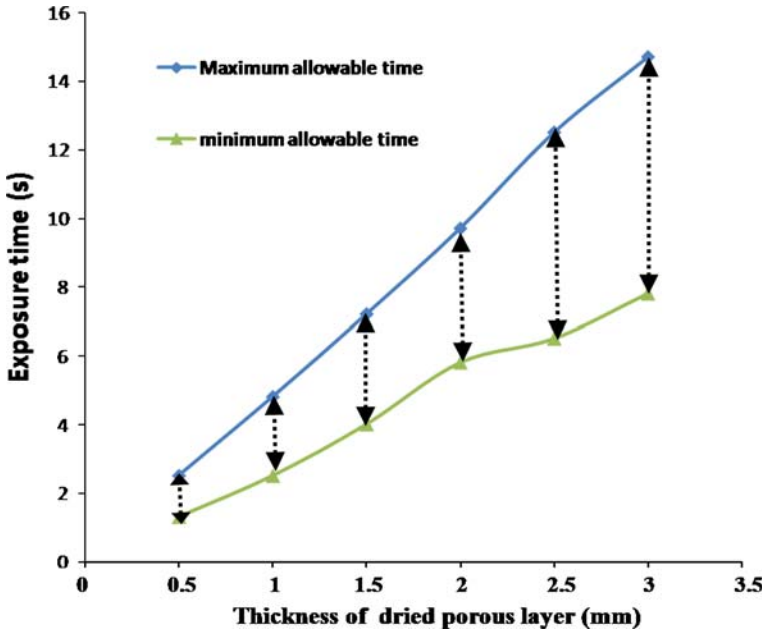

Fig. 8 Predictions of maximum and minimum exposure time for the formation of Si films

other words, the sensitivity of the process is higher at small thickness. The figure further can be used to find this maximum and minimum allowable time to reach to silicon thickness between 250 and 1500 μm.* From these data we can easily calculate the minimum and maximum allowable scanning speed of the substrate, the most critical parameter that should be optimized for each material with a given physical property (diffusivity) and thickness. These values can be used as starting points for performing the experiments.

4.2 Effect of He in the Sheath

This gas was injected to the maximum amount (200 slpm) in the sheath. He in the plasma state has much higher viscosity compared to other gases (Ref 20, 21); therefore, it decreases the level of flow turbulency and consequently the flow dynamics can be controlled more easily. Consequently, we may have more control over the film formation process. To understand better its effect, CFD simulations with Fluent^{TR} were performed and profiles of velocity were compared in this exercise. To obtain these profiles, the following assumptions are made:

1. K-ε turbulent model
2. Step wise change of transport properties of plasma gases with temperature (300 K $< T <$ 10,000 K).
3. Parabolic temperature and velocity profiles at the reactor inlet. They fit the energy and mass input into the reactor based on known operating conditions and plasma torch efficiencies.

*Note that the porosity of the dried layer before scanning by plasma flame is about 50%.

The results are shown in Fig. 9. According to this figure, with He (right-hand side) the fluid maximum velocity is 36 m/s while without He (left-hand side) the corresponding velocity is about 3 times more.

Another important aspect of this figure is that it shows the presence of four recirculation zones inside the reactor chamber. Two zones at the top and two at the bottom. These recirculations may explain the existence of impurities such as N and O in the form of a very thin layer on the surface of the film (Fig. 4b). In fact, as a result of these flow recirculations, the trace amounts of oxygen and nitrogen gases (that are present in the different parts of reactor) are transferred to the hot fabricated surface and react with the silicon.

5. Conclusion

An innovative method in thermal plasma process, namely plasma surface melting, is introduced and used for the ultra high rate fabrication (in the order of 150 cm^2/s) of uniform solid Si films of 250-700 μm thickness. The method consists in spreading a uniform layer of Si particles on a substrate (by suspension evaporation) and exposing the layer into a high heat flux source of plasma flame. Consequently, the effect of various process parameters was identified.

It was shown that, when the substrate distance decreases from 15 to 8 cm, the fabricated surface increases from 12 to 36 cm^2. By the injection of H_2 and He in the sheath and by decreasing the turbulence level in the plasma, it was possible to control the unwanted reactions and flow dynamics around the substrate and to produce uniform silicon films of crystalline structure with potential applications in the photovoltaic industry.

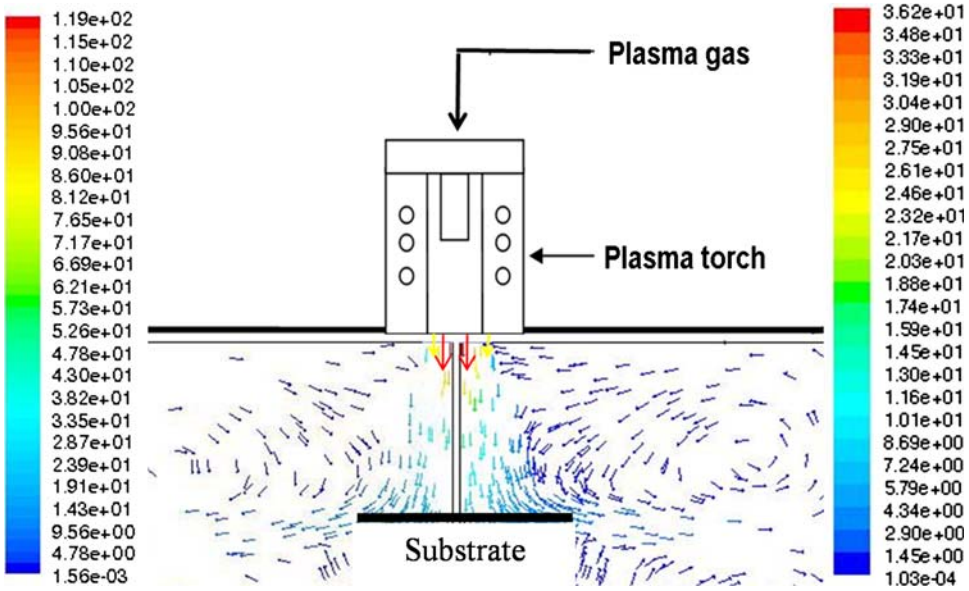

Fig. 9 Profiles of velocity colored by velocity magnitude inside the reactor chamber. (Left) Ar plasma (without He) and (right) with the presence of He

The results further indicate that the optimum conditions of film preparation is when the substrate scanning speed lies within a minimum and maximum exposure time of 5 and 12.5 s, respectively. At exposure times beyond these two limits, the film either does not form or is burned and is of low quality. At exposure times within these limits, the film is either porous or solid. These results were used to estimate the effective diffusivity within the porous layer to about 0.9 cm^2/s. Finally, using Fourier's law of conduction, a model has been developed to predict the diffusion of heat into the porous layer and to evaluate the minimum and maximum exposure times as a function of material properties and thickness of the porous layer. According to the model predictions, the sensitivity of the process increases when decreasing the thickness.

Acknowledgments

The authors highly appreciate the financial support of CEA (Grenoble, France) and NanoQuébec (Quebec, Canada). The support of the plasma laboratory technicians, Francis Barrette and of the mechanical technician Patrice Poulin through Plasma-Quebec grant is acknowledged. The collaboration of OPPUS group of the chemical engineering department for using their system for performing Fluent^{TR} simulations is well appreciated.

References

1. M. Gratzel, Photovoltaic and Photoelectrochemical Conversion of Solar Energy, *Philos. Trans. R. Soc. Lond. A Math. Phys. Eng. Sci.*, 2007, **365**(1853), p 993-1005
2. A. Goetzberger and C. Hebling, Photovoltaic Materials, Past, Present, Future, *Sol. Energy Mater. Sol. Cells*, 2000, **62**, p 1-19
3. A.V. Shah, H. Schade, M. Vanecek, J. Meier, S.E. Vallat, N. Wyrsch, U. Kroll, C. Droz, and J. Bailat, Thin-Film Silicon Solar Cell Technology, *Prog. Photovoltaics Res. Appl.*, 2004, **12**, p 113-142
4. Y. Nakano, S. Goya, T. Watanabe, N. Yamashita, and Y. Yonekura, High Deposition Rate of Microcrystalline Silicon Solar Cell by Using VHF PECVD, *Thin Solid Films*, 2006, **506-507**, p 33-37
5. Y.K. Chae, H. Ohno, K. Eguchi, and T. Yoshida, Ultrafast Deposition of Microcrystalline Si by Thermal Plasma Chemical Vapor Deposition, *J. Appl. Phys.*, 2001, **89**(12), p 8311-8315
6. G.M. Ferreira, A.S. Ferlauto, C. Chen, R.J. Koval, J.M. Pearce, C. Ross, C.R. Wronski, and R.W. Collins, Kinetics of Silicon Film Growth and the Deposition Phase Diagram, *J. Non-Cryst. Solids*, 2004, **338-340**, p 13-18
7. R. Koval, J. Koh, Z. Lu, L. Jiao, R.W. Collins, and C.R. Wronski, Performance and Stability of Si:H *p–i–n* Solar Cells with *i* Layers Prepared at the Thickness-Dependent Amorphous-to-Microcrystalline Phase Boundary, *Appl. Phys. Lett.*, 1999, **75**(11), p 1553-1555
8. Y. Xu, Z. Hu, H. Diao, Y. Cai, S. Zhang, X. Zeng, H. Hao, X. Liao, E. Fortunato, and R. Martins, Heterojunction Solar Cells with n-Type Nanocrystalline Silicon Emitters on p-Type c-Si Wafers, *J. Non-Cryst. Solids*, 2006, **352**, p 1972-1975
9. E. Vidal and R.P. Taylor, Thermal Plasma Synthesis of Ba-$Fe_{12}O_{19}$ (BaM) Films, *Plasma. Chem. Plasma Process.*, 2003, **23**(4), p 609-626
10. T. Sasaki, S. Fujikake, K. Tabuchi, T. Yoshida, T. Hama, H. Sakai, and Y. Ichikawa, Structural Study of p-Type μc-Si Layer for Solar Cell Application, *J. Non-Cryst. Solids*, 2000, **266-269**, p 171-175
11. B. Mostajeran Goortani, F. Gitzhofer, and E. Bouyer, Solid and Porous Film Formation from Particulate Materials by High Heat Flux Source, Patent (PCT/FR2007/001408), July 2007 (CEA, Grenoble, France and Sherbrooke University, Quebec, Canada)
12. M.I. Boulos, Purification of Metallurgical Grade Silicon, US Patent No. 4,379,777, April 12, 1983
13. D. Morvan and J. Amourous, Preparation of Photovoltaic Silicon by Purification of Metallurgical Grade Silicon with a Reactive Plasma Process, *Plasma. Chem. Plasma Process.*, 1981, **1**(4), p 397-418

14. F. Bourg, S. Pellerin, D. Morvan, J. Amouroux, and J. Chapelle, Study of an Argon–Hydrogen RF Inductive Thermal Plasma Torch Used for Silicon Deposition by Optical Emission Spectroscopy, *Sol. Energy Mater. Sol. Cells*, 2002, **72**, p 361-371
15. M. Benmansour, E. Francke, D. Morvan, J. Amouroux, and D. Ballutaud, In Flight Treatment of Metallurgical Silicon Powder by RF Thermal Plasma: Elaboration of Hydrogenated Silicon Deposit on a Substrate, *Thin Solid Films*, 2002, **403-404**, p 112-115
16. S.Zh. Tokmoldin, B.N. Mukashev, Kh.A. Abdullin, and Yu.V. Gorelkinskii, Hydrogen Interactions with Interstitial- and Vacancy-Type Defects in Silicon, *Phys. B: Condens. Matter*, 1999, **273-274**, p 204-207
17. B. Jagannathan, W.A. Anderson, and J. Coleman, Amorphous Silicon p-Type Crystalline Silicon Heterojunction Solar Cells, *Sol. Energy Mater. Sol. Cells*, 1997, **46**, p 289-310
18. R.H. Perry and D.W. Green, *Perry's Chemical Engineers' Handbook*, 7th ed., McGraw-Hill, 2007
19. H.S. Carslaw and J.C. Jaeger, *Conduction of Heat in Solids*, 2nd ed., Oxford University Press, 1986
20. A. Murphy, Transport Coefficients of Helium and Argon-Helium Plasmas, *IEEE Trans. Plasma Sci.*, 1997, **25**(5), p 809-814
21. J. Aubreton, M.F. Elchinger, V. Rat, and P. Fauchais, Two-Temperature Transport Coefficients in Argon–Helium Thermal Plasmas, *J. Phys. D: Appl. Phys.*, 2004, **37**, p 31-41